Journal of Theoretical Medicine, Vol. 6, No. 2, June 2005, 119–125

Taylor & Francis
Taylor & Francis Group

Dissecting the fine details of assembly of a $T = 3$ phage capsid

P.G. STOCKLEY*, A.E. ASHCROFT†, S. FRANCESE‡, G.S. THOMPSON§, N.A. RANSON¶, A.M. SMITH‖, S.W. HOMANS# and N.J. STONEHOUSE**

Astbury Centre for Structural Molecular Biology, University of Leeds, Leeds LS2 9JT, UK

The RNA bacteriophages represent ideal model systems in which to probe the detailed assembly pathway for the formation of a $T = 3$ quasi-equivalent capsid. For MS2, the assembly reaction can be probed *in vitro* using acid disassembled coat protein subunits and a short (19 nt) RNA stem-loop that acts as the translational operator of the replicase gene and leads to sequence-specific sequestration and packaging of the cognate phage RNA *in vivo*. Reassembly reactions can be initiated by mixing these components at neutral pH. The molecular basis of the sequence-specific RNA–protein interaction is now well understood. Recent NMR studies on the protein demonstrate extensive mobility in the loops of the polypeptide that alter their conformations to form the quasi-equivalent conformers of the final capsid. It seems reasonable to assume that RNA binding results in reduction of this flexibility. However, mass spectrometry suggests that these RNA–protein complexes may only provide one type of quasi-equivalent capsid building block competent to form five-fold axes but not the full shell. Work with longer RNAs suggests that the RNA may actively template the assembly pathway providing a partial explanation of how conformers are selected in the growing shell.

Keywords: RNA phage; Self-assembly; RNA scaffold

Msc: GEOMETRY

1. Introduction

It is now almost 20 years since the Harrison group reported the first atomic structure determination for a spherical virus particle, namely the capsid of Tomato Bushy Stunt Virus (TBSV) [1]. For the first time it was possible to see the details of the packing of a single type of capsomere, the TBSV coat protein (CP), into a quasi-equivalent, $T = 3$ spherical lattice [2].

The molecular details of the CP packing were dramatically different from the expectations based on the original theory of quasi-equivalence [2]. Instead of subtle differences in amino acid side chain orientations between quasi-equivalent subunits, the TBSV CP was seen to be organised into three distinct domains; a projecting, C-terminal (P) domain was the most radially distal feature and non-covalent interactions in this domain principally created CP dimers; connected to this domain via a short hinge region was a shell (S) domain composed of β-sheets in what is now classified as a Swiss-roll topology, which in turn was connected to an extended N-terminal domain. Crystallography of viral particles makes use of the non-crystallographic symmetry of the capsid to average the electron density maps created and thus improve resolution. An unfortunate consequence of this technique is that features within the virus that lack the symmetry of the outer coat are essentially averaged out of the final map. Thus, this first structure lacked any density that could be ascribed to the viral genomic RNA and large sections of the N-terminal domain that appeared to be intimately associated with it, consistent with its basic amino acid sequence. The $T = 3$ shell is created by differences in the orientation of the domains of the CP. In particular, the S domain in a third of the subunits is extended by an additional section of β-strand drawn from the N-terminal region. These strands being symmetrical within CP dimers and extending to the particle three-fold axes where they interdigitate with symmetry related

*Corresponding author. Tel./Fax: +44-113-343-3092. Email: stockley@bmb.leeds.ac.uk
† Email: a.e.ashcroft@leeds.ac.uk
‡ Email: simonafrancese@hotmail.com
§ Email: garyt@bmb.leeds.ac.uk
¶ Email: n.a.ranson@leeds.ac.uk
‖ Email: bmbams@bmb.leeds.ac.uk
Email: s.w.homans@leeds.ac.uk
** Email: n.j.stonehouse@leeds.ac.uk

Journal of Theoretical Medicine
ISSN 1027-3662 print/ISSN 1607-8578 online © 2005 Taylor & Francis Group Ltd
http://www.tandf.co.uk/journals
DOI: 10.1080/10273660500149869

features from other dimers creating what is termed a β-annulus, before being lost from the electron density map. The interdigitation of these extra strands of β-sheet has the result of altering the dihedral angle between S-domains creating a rather flat junction between them. In contrast, at the other 120 CP sites (60 dimers) the extra strands are not incorporated into the S domains but disappear immediately below the domain to interact with the RNA, allowing the S domains to collapse towards each other resulting in a curved junction between domains. The correct placement of curved and flat elements in the shell allowed the virus to define a closed shell of the correct size (~250 Å diameter) and symmetry.

These structural insights led to one of the first structure-based proposals for the assembly of a $T = 3$ shell based on formation of an initial assembly intermediate composed of a β-annulus, to which additional CPs could bind as appropriate quasi-equivalent conformers [3]. However, it has proved very difficult to arrive at a consensus about the molecular mechanisms underlying the self-assembly of such capsids, i.e. is there a defined assembly pathway or are multiple pathways followed until the structure is complete? In order to address these questions in more detail, we have chosen to work with the RNA bacteriophages, especially MS2, since their $T = 3$ capsids (figure 1) are composed of small, single domain CPs that form tightly locked non-covalent dimers (CP_2) that differ primarily in the orientation of a simple peptide loop, connecting the F and G β-strands, that defines the quasi-equivalent conformers at the particle symmetry axes. Since the interactions between the remainder of the CPs are mostly main chain contacts, the phages are closer to the original conception of quasi-equivalence than most viruses and are very easily manipulated. *In vivo* phage CPs selectively package their own RNA genomes even in the presence of closely related competitor phage RNAs [4], and the basis of this discrimination appears to be due to a sequence-specific CP_2–RNA interaction that occurs with stem-loop structures that can form within the genomic RNAs. Formation of these complexes accomplishes a number of biological functions. Initial sequestration of the start codon for the replicase cistron leads to

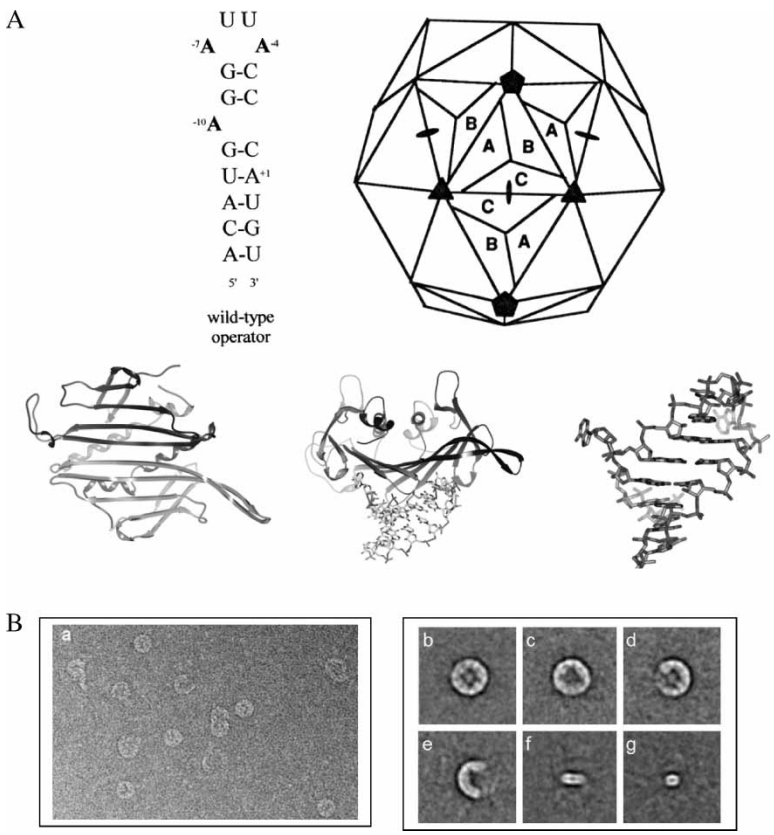

Figure 1. The components of the MS2 RNA bacteriophage system (A). From left to right along the top line: the secondary structure of the translational operator, TR; a cartoon showing the packaging of A/B and C/C dimers into the icosahedral lattice of the capsid, redrawn from [6]. Bottom line: Ribbon diagram of an AB dimer from the MS2 coat protein shell, viewed from the capsid interior. Subunit A is towards the bottom of the figure, with subunit B towards the top. A ribbon diagram of an AB dimer from the MS2 capsid complexed with its wild-type RNA stem-loop operator [6]; the A protein subunit is to the right of the dimer and the B subunit to the left. Complexed RNA is shown in stick format; the structure of the RNA stem-loop operator in isolation. Molecular figures created using SPOCK [13]. (B) (a) A raw image field of an MS2 *in vitro* reassembly reaction between TR and CP in neutral buffer in unsupported vitreous ice. Image taken on an FEI TF20 at 56,400 × magnification on a Gatan U4000SP CCD camera, binned to give a 2k × 2k image with 30 μm pixel size. ~2000 particles (27 micrographs, nominal defocus 1.2–2.9 μm) were interactively selected, their image phases flipped to give uniformly positive contrast, Fourier filtered between (15–350 Å) and normalised to a constant mean and std. deviation in SPIDER [14]. These images were then centred against a rotationally averaged total sum of the dataset and subjected to an MSA-based classification in IMAGIC [15]. Fifty class average views were calculated (~40 raw image views per class). Such classification shows intact MS2 $T = 3$ capsids (B b) recognisable MS2 capsids in various states of assembly (B e, d) and smaller unidentified assembly intermediates (B e–g).

translational repression of that gene product, and apparently marks the phage RNA for specific encapsidation. There are two major questions that we have been addressing with this system: What is the molecular basis of sequence-specific RNA recognition, and how does formation of this complex give rise to a $T = 3$ shell? The first question has to a large degree been answered using crystals of RNA-free capsids to soak in various RNA stem-loops that can penetrate to the interior of each capsid via the pores that exist at particle five-fold axes. There the RNA can bind to every CP_2 dimer creating an RNA–protein interaction that has the same symmetry as the outer protein shell, allowing the high resolution X-ray structures of the complexes to be determined by simple difference maps [5–10]. Our latest results addressing the second question are described below.

2. Results and discussion

2.1 The assembly pathway

DNA phages make capsid structures lacking genomic nucleic acid and then package the DNA post-assembly using specialised packaging machinery [11, 12]. Other viruses require higher order protein assemblies to form before they can trigger the assembly pathway. In order to investigate whether there are defined assembly intermediates in the MS2 system we used cryo-electron microscopy (cryo-EM) of reassembling mixtures (figure 1) to examine the species present in solution. The results suggest that when reassembly of the $T = 3$ capsid from CP_2 dimers is triggered by addition of the TR RNA stem-loop, an assembly process initiates that is akin to a crystallisation reaction. The shell appears to grow continuously from this initial complex by a series of low order reactions.

This assembly pathway is similar to that proposed for the close homologue of TBSV [3], namely Turnip Crinkle Virus, although in that case the formation of the β-annular structure, consisting of three CP dimers in the C/C quasi-equivalent conformation, automatically creates binding sites for the more curved A/B dimers to add at the edges, and simultaneously defines the positions of the next particle three-fold axes, and subsequent β-annuli, via the symmetry related "arms" in each C-type subunit. The molecular basis of defining the capsid architecture in the case of the RNA phages, however, must be different; the initial RNA–protein interaction being entirely within a single CP dimer. Clearly, it is important to determine what happens in molecular terms when the TR-CP dimer forms in order to understand higher order assembly.

2.2 Probing the effects of complex formation on TR and a CP dimer

NMR [16], fluorescence spectroscopy [23, 28] and biochemical structure probing [27] all suggest that the unliganded TR RNA exists in solution as an ensemble of differing conformers and that distinct states can occur in response to changes in solution conditions. In particular, NMR suggests that the dominant conformer is one in which the bulged A (A-10) on the 5′ leg of the stem intercalates between neighbouring base pairs imparting a distinct kink on the A-helical axis of the RNA. This is a very different conformer than the one that ultimately is generated when the TR binds to the CP in the context of a capsid. In that case (figure 1), A-10 is extruded from the stem, allowing a fully A-helical structure to occur, and gets inserted into an adenine binding pocket on one protein subunit; the symmetry related contact to that made on the half of the dimer with the A-4 from the loop. Thus, there are major rearrangements of the stem and the loop residues to allow these sequence specific RNA–protein contacts to occur.

Similarly, the unliganded CP dimer exists as a conformational ensemble. When assembled in the $T = 3$ shell, each CP subunit can take up one of three distinct quasi-equivalent conformations that primarily involve the FG-loop sequence. In C/C-type dimers, this loop is in an extended conformation and these loops interdigitate at the particle three-fold axes between loops in a fairly similar conformation coming from A-type subunits. In sharp contrast, at B-type subunits this identical peptide sequence folds back towards the globular body of the protein. These loops come together at the particle five-fold axes. It would appear that the answer to the question of how the molecular assembly pathway is determined lies in understanding how these loop conformations are selected. X-ray crystallography [17] showed that residue Pro78 was in a *trans* configuration in A and C FG-loops but adopted the *cis* configuration in B subunits, suggesting that it was the molecular switch controlling this event. This would be consistent with the conservation of this residue in a large number of phage CP sequences. However, we found that on replacement of the Pro with Asn, $T = 3$ capsids still formed with similar efficiency. The structure of the mutant capsid showed that all Asn residues were in the *trans* configuration and that in B subunits the FG-loop was folded similarly to wild-type protein with Asn being able to mimic very closely the *cis* Pro [18]. Substitution of this mutation into an infectious cDNA clone, however, resulted in a non-viable phage, suggesting that the conservation of the Pro78 residue is due to another vital function. These residues from different subunits line the pore at the particle five-fold axes and may be important during extraction of the genomic RNA during infection, or as part of the binding site for the maturation (A) protein [19], that is present at a level of one copy per particle and serves to bind the phage to the pili of target bacteria.

In order to examine how FG-loop conformations form we have used NMR to examine the dynamic behaviour of the CP in solution. This is not possible with wild-type CP that would self-assemble at NMR concentrations. Instead we have used a non-assembling mutant, Trp82Arg, that contains a substitution within the FG-loop. The X-ray structure of this protein with and without bound TR has previously been reported [20]. The bulk of the protein is unaltered from wild-type but the FG-loops were not

visible due to conformational flexibility. Stopped-flow fluorescence RNA-CP binding assays show that despite the sequence change the TR affinity for this protein is identical to that of wild-type (Lago, unpublished). Following assignment of the NMR spectrum of Trp82Arg, we probed dynamic motions within the CP using measurements of $^{1}H-^{15}N$ T1/T2 relaxation rates and heteronuclear nOe measurements [21, 22]. These techniques probe molecular motion on the sub-nanosecond to microsecond scale. The preliminary nOe result is shown in figure 2(A). No high frequency ps–ns motions are detected within the main secondary structure elements of the trp82arg-CP dimer consisting of the eight stranded β sheets and the C-terminal helices. However, such motions are significant within the loops linking these structural elements, especially in the F–G loops and the ends of the β strands leading to them. Thus, the primary RNA-binding site comprising the core β-sheet is relatively stable but the sites at which conformational changes must take place to allow capsids to form are very dynamic. Furthermore, the extension of these motions along the β-strands allows this effect to overlap, in part, with the RNA-binding site. It is tempting to speculate that RNA binding and FG-loop conformations are in some sense coupled. This would be consistent with other stopped-flow experiments that show that, although the bulk of CPs bind RNA in a diffusion limited reaction, a fraction of the unliganded CP

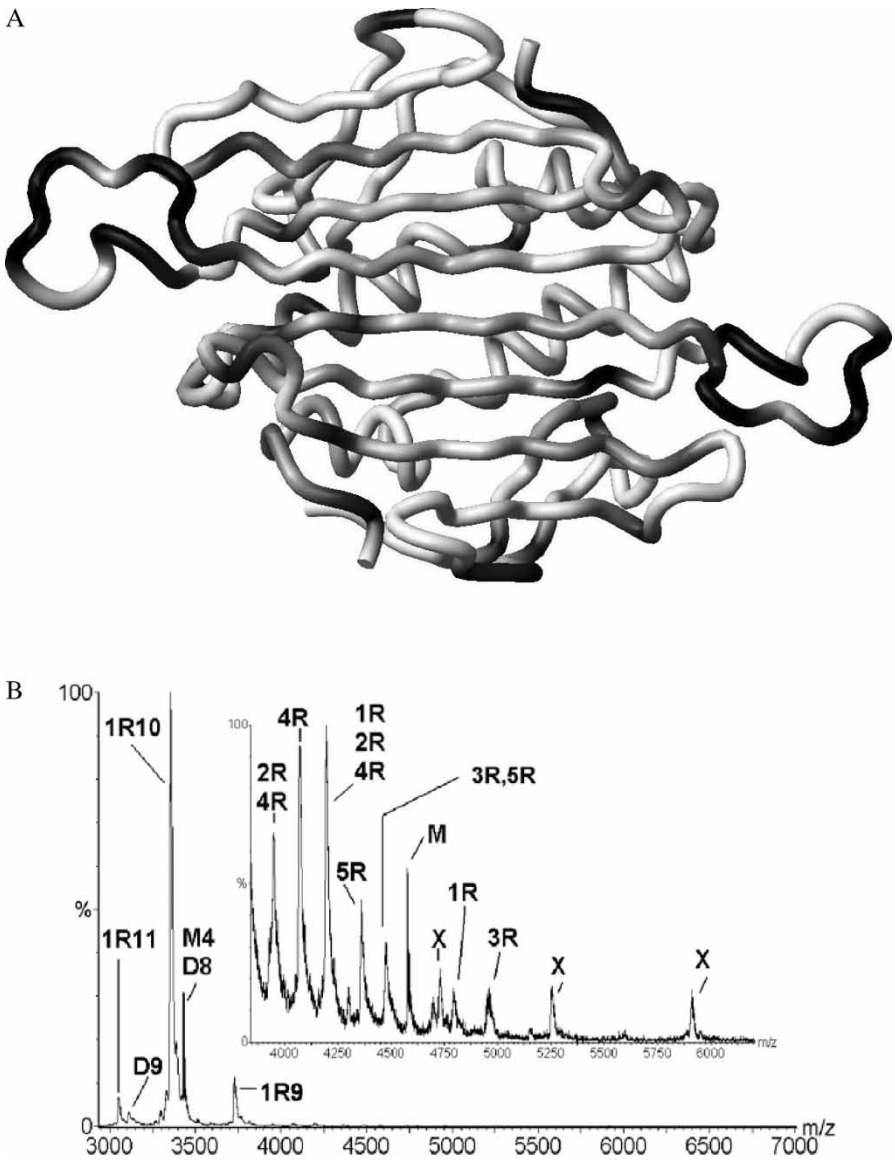

Figure 2. Characterisation of the TR-CP_2 complex. (A) Figure showing dynamics on ns–ps timescales for the backbone of unliganded trp82org. The image shows a tubes representation of the backbone of trp82org [PDB code: 1MSC] with $^{1}H-^{15}N$ hetero-nuclear nOes shown by shading from white to black with increasing mobility. White represents an nOe of ~0.8–0.9 (the theoretical maximum indicating rigidity) whereas the most intense black represents an nOe of 0.13, indicating a significant motion. (B) Mass spectrum of MS2 coat protein mixed with TR (in 40 mM aqueous ammonium acetate), acquired using nanoflow ES Q-Tof MS with a capillary voltage of 900–1200 V, a cone voltage of 90 V, and MCP 2400–2700V. M = CP, D = CP_2, nR = $[CP_2 - TR]_n$, X = $[CP_3 - TR]$. The number immediately after M, R, D, etc. refers to the charge state of these ions. The insert shows the *m/z* 3500–6500 region expanded.

molecules are unable to bind to the RNA until they have undergone a conformational change [23].

What might the CP conformers that are competent to bind TR look like and how might they contribute to the assembly pathway? We are working to determine the answer to the first part of this question using NMR but have been using Q-Tof mass spectrometry to probe the second part. Figure 2(B) shows the mass spectrum of a TR/wild-type CP reassembly reaction. Dominant peaks are seen for the TR-CP dimer complex (1R9, 1R10 and 1R11). However, at higher *m*/*z* values, there are a series of low intensity peaks corresponding to the formation of higher order multimers of this complex, up to and including $(CP_2\text{-}TR)_5$. We have not seen species of higher stoichiometry in these experiments, suggesting that only a complex corresponding to a fully formed five-fold axis can form in such mixtures. This in turn suggests that there is a preference for forming an A/B CP dimer when TR binds, since only A/B dimers are found around five-fold axes.

Such pentamers of dimers have been proposed previously as an intermediate during the assembly of the $T = 3$ shell of CCMV [24]. Is it reasonable to conclude, therefore, that a similar pathway is followed by the RNA phages? A number of observations suggest that this interpretation needs to be treated with care. The reassembly reactions in which $(CP_2\text{-}TR)_5$ is observed at very low levels is triggered by the TR stem-loop encompassing just 19 nt present at a stoichiometric ratio with the CP dimer. This entire RNA fragment binds within a single CP dimer. Although the NMR data suggest that this might then result in fixing, or promoting, a defined conformation for the FG-loops, it does not readily explain how the contacts to the next CP dimer are regulated. Both mass spectrometry and stopped-flow fluorescence [23] suggest that CP_2-TR complexes are unexpectedly stable for an assembly initiation trigger. In the context of the phage genome the TR sequence is only transiently folded into the operator stem-loop [25], and there is only one copy of the operator sequence per $\sim$3500 nt. It is therefore important to consider what effect the genomic RNA has on the kinetics and pathway of the assembly reaction. Longer RNA fragments will clearly extend outside the edges of the initially bound CP dimer. Presumably, in the final capsid, each dimer is able to make non-sequence-specific contacts to the RNA. This seems to be consistent with the recent cryo-EM reconstruction of the wild-type phage [26].

2.3 The roles of phage RNA in the assembly reaction

In order to probe the effects of longer RNA fragments on the phage CP assembly reaction *in vitro*, we produced two longer RNAs, each of 31 nt, encompassing the TR sequence at either their 5′ or 3′ ends, i.e. with 12 nt extensions in either the 5′ or 3′ direction. These additional RNA sequences match the natural genomic sequences but are not large enough to encompass any of the predicted additional elements of secondary structure, such as the translational termination stem-loop for the coat protein that lies 5′ to the TR operator (figure 3). Neither is long enough to mimic the interactions of the TR with a second CP dimer suggesting that they only probe a potential role for the RNA "linking" capsomeres. Reassembly reactions were then carried out by titrating a fixed amount of the RNAs with increasing ratios of the CP_2 and the products examined after 1 h by gel electrophoresis on either agarose gels to visualise the capsid-sized products or agarose-acrylamide gels to examine the lower molecular weight species being formed (figure 3(B) and (C)). The results suggest that the longer RNA fragments all support the assembly reaction and that $T = 3$ capsids are the end result of the process. However, the loss of free RNA occurs at lower protein concentrations with the longer RNAs and there are distinct differences in the ability of the RNA–CP_2 complexes that form to recruit additional subunits and form higher order species. The 3′ extension RNA in particular seems to impede progress to higher order species, even compared to the TR fragment. In contrast, the 5′ extension results in CP dimer-RNA complexes that readily get converted into species no longer able to enter the gel. Remarkably, they also generate an additional RNA–protein species that migrates within the gel (figure 3(C)). Interestingly, the TR stimulated reaction generates species that migrate slower than the $T = 3$ capsid in agarose gels (figure 3(C)). At higher protein concentrations, these species tend to disappear and be replaced by the expected capsid product, whereas the longer RNAs do not show this behaviour. Analysis of stoichiometric reassembly reactions with these RNAs using a gel filtration column coupled to a light scattering detector (figure 3(D)) confirms the electrophoresis results. For TR and the 3′ extension RNA the principal products are the RNA–CP_2 complex and the $T = 3$ capsid. In contrast, the 5′ extension RNA leads to the appearance of intermediate species in the column with apparent masses of 150 and 350 kDa.

We interpret these data to mean that the phage genomic RNA plays an active role in the assembly pathway, i.e. it is not just a passive cargo to be packaged, and that this is sensitive to the sequence/structure of the RNA outside the TR operator. This would make sense because it would allow the RNA to capture and steer additional CP dimers into the correct position to make the next contact with the dimer bound to TR. It is interesting to speculate how far this role of RNA in the assembly pathway extends, i.e. does it function only at the start of the assembly reaction in order to establish an essential intermediate, or does it act throughout the assembly reaction to define the pathway? Both options imply structural and sequence constraints on the folding of the genomic RNA. We are now testing these ideas by combining mass spectrometry and cryo-EM analysis with the gel filtration/light scattering assay shown in figure 3 in order to determine the precise nature of the intermediate species seen with the 5′ extended TR [27,28].

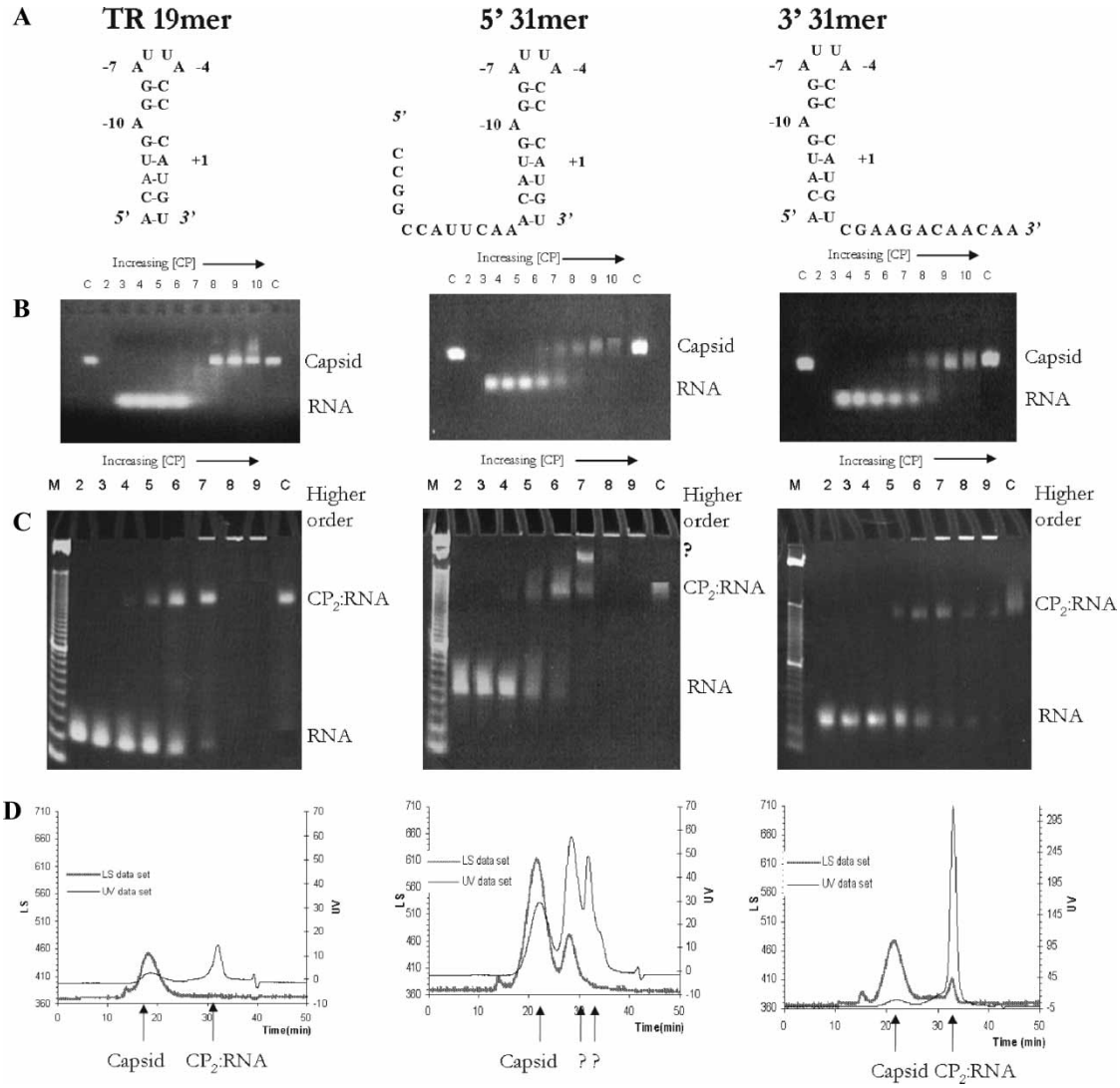

Figure 3. The role(s) of RNA in the phage. (A) Sequences of TR, a 31-mer RNA extending 5′ (5′ 31mer) and a 31-mer RNA extending 3′ (3′ 31mer). (B) Agarose gel retardation assay of reassembly. Lanes 1 and 11 = WT capsids used as a reference. Lanes 3–10 = RNAs at 1 μM with 0, 0.1, 0.2, 0.5, 1, 2, 4 and 5 μM CP_2. All of the RNAs can promote capsid formation, but this happens at lower [CP_2] for the longer RNAs. (C) Agarose–Acrylamide gel retardation assay of reassembly. M = 10 bp DNA ladder. Lanes 2–9 = RNAs at 1 μM with 0, 0.1, 0.2, 0.5, 1, 2, 4 and 5 μM CP_2. Lane 10 = 1 μM RNA with 2 μM CP_2W82R (non-assembling mutant) as control. Reassembly with the 5′ 31mer RNA shows the presence of species (?) larger than the RNA–CP_2 complex (but smaller than the final product) that are not seen with the other RNAs. (D) Static light scattering analysis of reassembly. Reassembly with the 5′ 31mer RNA shows the presence of species larger than the RNA–CP_2 complex (but smaller than capsids) that are not seen with the other RNAs. Black lines are UV traces; light grey light scattering signal.

Acknowledgements

We thank Wilf Horn for the structural images shown in figure 1 and Lars Lijlas and Kaspars Tars (Uppsala), David Peabody Albuquerque and Simon Phillips for continued helpful discussions of the phage system and their continued collaborations on this project. We are grateful to The Leverhulme Trust, The Wellcome Trust and the UK BBSRC for financial support.

References

[1] Winkler, F.K., Schutt, C.E., Harrison, S.C. and Bricogne, G., 1977, Tomato bushy stunt virus at 5.5 Å resolution. *Nature*, **265**, 509–513.

[2] Caspar, D. and Klug, A., 1962, Physical principles in the construction of regular viruses. *Cold Spring Harbor Symposium* (New York: The Cold Spring Harbor Laboratory), **XXVII**.

[3] Sorger, P.K., Stockley, P.G. and Harrison, S.C., 1986, Structure and assembly of turnip crinkle virus. II: Mechanism of reassembly *in vitro*. *J. Mol. Biol.*, **191**, 639–658.

[4] Ling, C.M., Hung, P.P. and Overby, L.R., 1970, Independent assembly of Qβ and MS2 phages in doubly infected *E. coli*. *Virology*, **40**, 920–929.

[5] Valegård, K., Murray, J.B., Stockley, P.G., Stonehouse, N.J. and Liljas, L., 1994, Crystal structure of a bacteriophage RNA coat protein operator system. *Nature*, **371**, 623–626.

[6] Valegård, K., Murray, J.B., Stonehouse, N.J., van den Worm, S., Stockley, P.G. and Liljas, L., 1997, The three dimensional structures of two complexes between recombinant MS2 capsids and RNA operator fragments reveal sequence specific protein–RNA interactions. *J. Mol. Biol.*, **270**, 724–738.

[7] Convery, M.A., Rowsell, S., Stonehouse, N.J., Ellington, A.D., Hirao, I., Murray, J.B., Peabody, D.S., Phillips, S.E. and Stockley,

P.G., 1998, Crystal structure of an RNA aptamer–protein complex at 2.8 Å resolution. *Nat. Struct. Biol.*, **5**, 133–139.

[8] Rowsell, S., Stonehouse, N.J., Convery, M.A., Adams, C.J., Ellington, A.D., Hirao, I., Peabody, D.S., Stockley, P.G. and Phillips, S.E.V., 1998, Crystal structures of a series of RNA aptamers complexed to the same protein target. *Nat. Struct. Biol.*, **5**, 970–975.

[9] Grahn, E., Stonehouse, N.J., Murray, J.B., van den Worm, S., Valegård, K., Fridborg, K., Stockley, P.G. and Liljas, L., 1999, Crystallographic studies of RNA hairpins in complexes with recombinant MS2 capsids: Implications for binding requirements. *RNA*, **5**, 131–138.

[10] Grahn, E., Stonehouse, N.J., Adams, C.J., Fridborg, K., Beigelman, L., Matulic-Adamic, J., Warriner, S.L., Stockley, P.G. and Liljas, L., 2000, Deletion of a single hydrogen bonding atom from the MS2 RNA operator leads to dramatic rearrangements at the RNA-coat protein interface. *Nucleic Acids Res.*, **28**, 4611–4616.

[11] Gossard, D.C. and King, J., 2005, Lattice transformations and subunit conformational changes in phage capsid maturation. *J. Theor. Med.*, 99–105, this volume.

[12] Wood, J.P.A., Capaldi, S.A., Robinson, M.A., Baron, A.J. and Stonehouse, N.J., 2005, RNA multimerisation in the DNA packaging motor of bacteriophage ϕ29. *J. Theor. Med.*, 127–134 this volume.

[13] Christopher, J.A., 1997 *SPOCK: The Structural Properties Observation and Calculation Kit*, Programme manual.

[14] Frank, J., Radermacher, M., Penczek, P., Zhu, J., Li, Y., Ladjadj, M. and Leith, A., 1996, SPIDER and WEB: processing and visualization of images in 3D electron microscopy and related fields. *J. Struct. Biol.*, **116**, 190–199.

[15] van Heel, M., Harauz, G., Orlova, E.V., Schmidt, R. and Schatz, M., 1996, A new generation of the IMAGIC image processing system. *J. Struct. Biol.*, **116**, 17–24.

[16] Borer, P.N., Lin, Y., Wang, S., Roggenbuck, M.W., Gott, J.M., Ulhenbeck, O.C. and Pelczer, I., 1995, Proton NMR and structural features of a 24-nucleotide RNA hairpin. *Biochemistry*, **34**, 6488–6503.

[17] Golmohammadi, R., Valegård, K., Fridborg, K. and Liljas, L., 1993, The refined structure of bacteriophage MS2 at 2.8 Å resolution. *J. Mol. Biol.*, **234**, 620–639.

[18] Stonehouse, N.J., Valegard, K., Golmohammadi, R., van den Worm, S., Walton, C., Stockley, P.G. and Liljas, L., 1996, Crystal Structures of MS2 capsids with mutations in the subunit FG loop. *J. Mol. Biol.*, **256**, 330–339.

[19] Hill, H.R., Stonehouse, N.J., Fonseca, S.A. and Stockley, P.G., 1997, Analysis of phage MS2 coat protein mutants expressed from a reconstituted phagemid reveals that proline 78 is essential for viral infectivity. *J. Mol. Biol.*, **266**, 1–7.

[20] Ni, C.Z., Syed, R., Kodandapani, R., Wickersham, J., Peabody, D.S. and Ely, K.R., 1995, Crystal structure of the MS2 coat protein dimer: implications for RNA binding and virus assembly. *Structure*, **3**, 255–263.

[21] Palmer, III A.G., 2001, NMR probes of of molecular dynamics: overview and comparison with other techniques. *Ann. Rev. Biophys. Biomol. Struct.*, **30**, 129–155.

[22] Kalverda, A.P., Thompson, G.S. and Turnbull, W.B., The importance of protein structural dynamics and the contribution of NMR spectroscopy. *Encyclopedia of Genetics, Genomics, Proteomics and Bioinformatics* (Wiley Interscience) in press.

[23] Lago, H., Parrott, A.M., Moss, T., Stonehouse, N.J. and Stockley, P.G., 2001, Probing the kinetics of formation of the bacteriophage MS2 translational operator complex: identification of a protein conformer unable to bind RNA. *J. Mol. Biol.*, **305**, 1131–1144.

[24] Zlotnick, A., Aldrich, R., Johnson, J.M., Ceres, P. and Young, M.J., 2000, Mechanism of capsid assembly for an icosahedral plant virus. *Virology*, **277**, 450–456.

[25] Berkhout, B. and van Duin, J., 1985, Mechanism of translational coupling between coat protein and replicase genes of RNA bacteriophage MS2. *Nucleic Acids Res.*, **13**, 6955–6967.

[26] Koning, R., van den Worm, S., Plaisier, J.R., van Duin, J., Pieter Abrahams, J. and Koerten, H., 2003, Visualization by cryo-electron microscopy of genomic RNA that binds to the protein capsid inside bacteriophage MS2. *J. Mol. Biol.*, **332**, 415–422.

[27] Talbot, S.J., Medina, G., Fishwick, C.W.G., Haneef, I. and Stockley, P.G., 1991, Hyper-reactivity of adenines and conformational flexibility of a translational repression site. *FEBS Lett.*, **283**, 159–164.

[28] Parrott, A.M., Lago, H., Adams, C.J., Ashcroft, A.E., Stonehouse, N.J. and Stockley, P.G., 2000, RNA aptamers for the MS2 bacteriophage coat protein and the wild-type RNA operator have similar solution behaviour. *Nucleic Acids Res.*, **28**, 489–497.